Environmental Science
Water Research & Technology

PAPER

View Article Online
View Journal | View Issue

CrossMark click for updates

Cite this: *Environ. Sci.: Water Res. Technol.*, 2015, **1**, 874

Antibacterial behavior of halloysite nanotubes decorated with copper nanoparticles in a novel mixed matrix membrane for water purification

Linlin Duan,[a] Qianqian Zhao,[a] Jindun Liu[a] and Yatao Zhang*[ab]

Received 27th May 2015,
Accepted 12th August 2015

DOI: 10.1039/c5ew00140d

rsc.li/es-water

Poly(4-vinylpyridine) (P4VP) with various molecular weights was grafted onto halloysite nanotubes (HNTs) *via* reverse atom transfer radical polymerization (RATRP). Then copper nanoparticles (Cu NPs) were loaded onto the surface of HNTs by complexation and reduction (Cu NPs@HNTs). Finally, a novel mixed matrix membrane, polyethersulfone (PES) ultrafiltration membrane, containing Cu NPs@HNTs was fabricated *via* the classical phase inversion method. The results showed that the pure water flux of the hybrid membrane was greatly enhanced, and the maximum could reach as high as 212 L m^{-2} h^{-1}. The contact angle and atomic force microscopy (AFM) results indicated that the hydrophilicity of the prepared membranes was improved and the surface became smoother, compared with the virgin membranes. Importantly, the antibacterial test indicated that the hybrid membranes showed good antibacterial activity against *E. coli* with a high bacteriostasis rate of 94.5%.

Water impact

Many areas of groundwater and surface water are now contaminated with microbes that have an adverse effect on health. Waterborne diseases and water-caused health problems are mostly due to inadequate and incompetent management of water resources. To address the above issue, the present work provides a novel ultrafiltration membrane functionalized by halloysite nanotubes decorated with copper nanoparticles. Compared with regular UF membranes, the functionalized membranes showed high antibacterial potential and could be used for treatment of direct or indirect potable water.

Published on 12 August 2015. Downloaded on 16/01/2016 12:12:48.

1. Introduction

Polyethersulfone (PES) with excellent chemical resistance, good thermal stability, oxidation resistance and mechanical properties is widely used as a membrane material.[1–3] However, the hydrophobic character limits its applications, because this could lead to serious membrane fouling.[4] Fouling is a significant challenge for membrane filtration, which could diminish the separation capabilities and increase the cost for membrane cleaning and replacement.[5] Thus, it is very necessary to improve the surface hydrophilicity of PES membranes, usually by incorporation of inorganic nanomaterials into PES membranes to fabricate mixed matrix membranes. There are two main approaches for producing mixed matrix membranes: blending the nanomaterials into the membrane matrix and coating the nanomaterials on the surface of the membrane.[6,7] The former approach is simpler because the nanomaterials are added to the membrane casting solution, avoiding some significant undesirable changes in membrane permeability due to pore narrowing or plugging. Several inorganic nanomaterials have been used to modify PES membranes, including TiO_2,[6,7] SiO_2,[8] Al_2O_3,[9] halloysite nanotubes (HNTs),[10] and carbon nanotubes (CNTs).[11] The above studies show that it is very effective in the improvement of the membrane antifouling performance *via* good dispersion of inorganic nanoparticles in the polymer matrix.

Biofouling, initiated by bacteria that attach and grow on the surface of membranes, is another hindrance to the application of membranes. Recently, copper nanoparticles (Cu NPs) have been considered as a promising antibacterial material because of their high surface-to-volume ratio and antimicrobial activity against a wide range of microorganisms including bacteria, fungi, algae and viruses.[12] The antibacterial mechanisms of Cu NPs could be explained by the fact that Cu NPs could attach to the bacterial cell membrane, causing structural changes or functional damage and inhibiting its growth, leading to cell death.[13] However, Cu NPs are likely to aggregate, which could decrease their antibacterial activity. Therefore, most nanoparticles are usually loaded on a type of inorganic carrier to improve their dispersion.[14–16] HNTs are a kind of natural nanotube with

[a] *School of Chemical Engineering and Energy, Zhengzhou University, Zhengzhou 450001, PR China. E-mail: zhangyatao@zzu.edu.cn; Fax: +86 371 67739348; Tel: +86 371 67781734*
[b] *UNESCO Centre for Membrane Science and Technology, School of Chemical Engineering, University of New South Wales, Sydney, NSW 2052, Australia*

This journal is © The Royal Society of Chemistry 2015

Published on 12 August 2015. Downloaded on 16/01/2016 12:12:48.

good hydrophilicity and hollow nanotubular structure. Compared with other nanomaterials, such as CNTs, HNTs are readily obtainable, far less expensive and more easily modified. Their novel physical and chemical properties provide opportunities for advanced applications in many fields.[17–19] As we know, Cu NPs are easier to remove if they are simply deposited on the surface of HNTs without any chemical interaction. In view of this, it will be better to anchor Cu NPs onto the surface of HNTs *via* a chemical reaction. In our previous work, poly(4-vinylpyridine) (P4VP) has been used to bind copper ions, because the nitrogen atom has a lone pair or lone pairs of electrons, and could bind a proton or metal ions through electron pair sharing to form a complex.[20] Atom transfer radical polymerization (ATRP) is usually used for the polymerization of vinyl monomers in a controlled/"living" manner onto the surfaces of nanoparticles.[21] For example, P4VP brushes have been grafted onto the surfaces of HNTs *via* surface-initiated atom transfer radical polymerization (SI-ATRP).[22] However, for ATRP, halide species RX are toxic and not easily handled or obtained, and the catalysts Mt^n/L_X are easily oxidized by oxygen in air.[23] To overcome these drawbacks, reverse atom transfer radical polymerization (RATRP) has recently been explored. Unlike ATRP, for the RATRP process, a conventional radical initiator, 2,2′-azobisisobutyronitrile (AIBN), is used instead of an organic halide initiator RX. The metal catalyst (CuCl) was replaced with a more stable catalyst ($CuCl_2$).[23]

In this study, copper nanoparticle-supported halloysite nanotubes (Cu NPs@HNTs) were fabricated *via* surface-initiated reverse atom transfer radical polymerization. Then, a novel PES mixed matrix ultrafiltration membrane with enhanced antibacterial activity and high flux was prepared by blending with Cu NPs@HNTs *via* a phase inversion method.

2. Materials and methods

2.1 Materials

Halloysite nanotubes (HNTs) were refined from clay minerals in Henan province, China. Cyclohexanone was distilled under reduced pressure and stored over molecular sieves (4A) to obtain anhydrous cyclohexanone. 4-Vinylpyridine (4VP) was dried over CaH_2 at 100 °C for 12 h and distilled under vacuum. Copper chloride ($CuCl_2$) was dried at 100 °C to remove the water. AIBN was recrystallized under methanol. PES (Ultrason E6020P with Mw = 58 kDa) was obtained from BASF, Germany. Bovine serum albumin (BSA, Mw = 67 000 g mol^{-1}) was purchased from Merck, Germany. The test strains, *E. coli.* (8099), used for this study were provided by the College of Public Health of Zhengzhou University, China. All the other chemicals (analytical grade) were obtained from Tianjin Kermel Chemical Reagent Co., Ltd., and used without further purification. The water used was deionized water.

2.2 Preparation of Cu NPs@HNT nanocomposites

In this study, Cu NPs@HNTs were prepared *via* reverse atom transfer radical polymerization. A schematic illustration of the overall preparation process of Cu NPs@HNTs is shown in Fig. 1a. The microstructures of HNTs and Cu NPs@HNTs were observed by TEM and the results are shown in Fig. 1b and c.

HNTs modified by CPS. HNTs should be treated by drying at 400 °C for 5 h to remove the adsorbed water molecules in advance. The dried HNT powder (6.0 g), 3-chloropropyl triethoxysilane (CPS, 9.0 g) and toluene (100 mL) were stirred ultrasonically for 30 min to obtain a homogeneous mixture. Then, triethylamine (1.0 mL), as a catalyst, was put in the above mixture. After reaction for 48 h at 135 °C, the product was collected by centrifugation and washed with isopropanol 4–5 times and was obtained by drying under vacuum at 60 °C.

P4VP grafted HNTs. HNTs modified by CPS (1.50 g), 4-vinylpyridine, (4VP, 5.26 g), anhydrous $CuCl_2$ (0.067 g) and 2,2′-bipyridine (BPy, 0.16 g) were mixed in 40 mL of cyclohexanone with the aid of ultrasonication in a water bath (KH-100, 100 W). The mixture was subsequently diluted and vacuum-filtered twice to make sure that the solution was exposed to nitrogen atmosphere. After reaction for 10 min at 75 °C, AIBN/cyclohexanone solution (20 mL, containing 0.082 g of AIBN) was dropwise added into the above mixture, followed by reaction for a certain period at 75 °C. The resulting mixture was centrifuged, and then the obtained precipitate was washed with acetone several times and dried under vacuum at 60 °C.

Cu NPs@HNT nanocomposites. $CuCl_2{\cdot}2H_2O$, P4VP grafted HNTs and 40 mL of deionized water were put into a container containing a magnetic stir bar. After stirring for 1 h, the container was moved into a table concentrator and shaken for 24 h at 60 °C. Then, the product was collected by centrifugation and dried under vacuum at 60 °C. Finally, the above product was dispersed in 100 mL of deionized water and the mixture was purged with nitrogen for 15 min, followed by addition of $NaBH_4$ solution (0.001 g mL^{-1}) dropwise. After purging with nitrogen for 15 min, the flask was sealed and refluxed under nitrogen for 24 h at 100 °C. The resulting mixture was centrifuged, and then the obtained precipitate was washed with deionized water and ethanol once and 3 times, respectively. After that, the product was immersed in oleic acid, making the solid inactive. At last, the inactivated Cu NPs@HNTs were washed with ethanol several times and dried under vacuum at 50 °C.

2.3 Preparation of PES mixed matrix membranes

All the membranes were prepared by the classical phase inversion method. A casting solution of PES dissolved in DMAC was prepared using PVP as the pore former by stirring at room temperature. After the formation of a homogeneous solution, Cu NPs@HNTs were added into the casting solution. In order to achieve optimal dispersion of inorganic nanomaterials in the polymer solution, vigorous stirring was required for at least 8 h.

The casting solution is composed of PES (20 wt%, by weight of the solution), DMAC (71.2 wt%, by weight of the

Published on 12 August 2015. Downloaded on 16/01/2016 12:12:48.

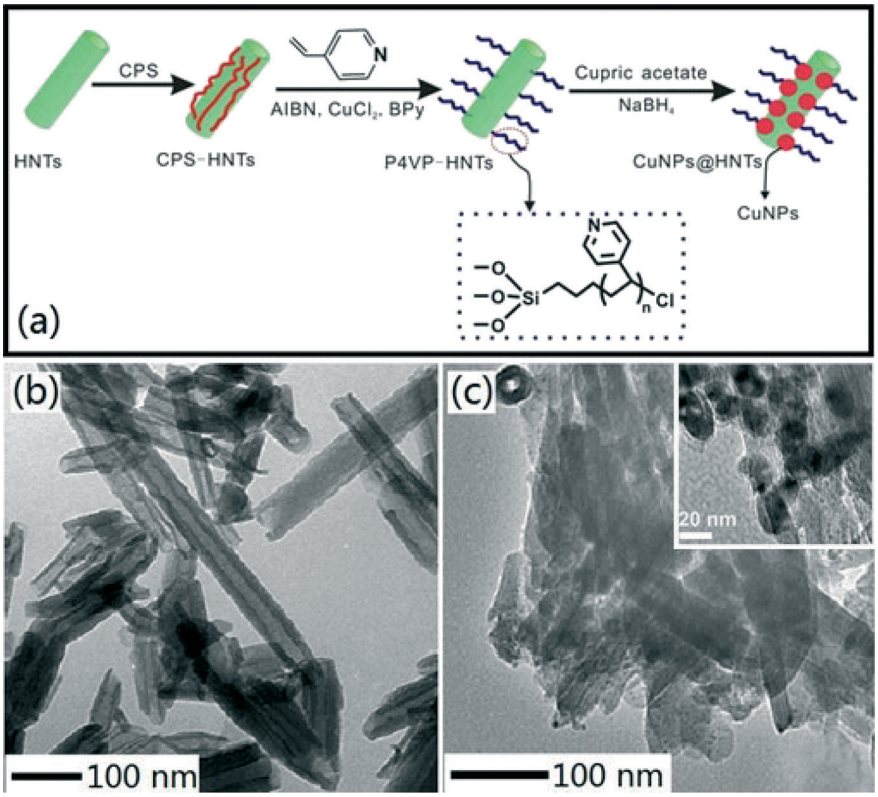

Fig. 1 (a) Schematic illustration of the overall preparation process of Cu NPs@HNTs; TEM images of (b) HNTs and (c) Cu NPs@HNTs (insert, higher magnification).

solution), PVP (8 wt%, by weight of the solution), acetone (0.8 wt%, by weight of the solution), and different Cu NPs@HNT contents (0–3 wt%, by weight of PES). The obtained homogeneous solution was degassed under vacuum and cast on a glass substrate by a casting knife with a thickness of 0.1 mm. Subsequently the glass substrate was immersed in a coagulation bath (deionized water, 20 °C) for precipitation. The prepared membranes were kept in deionized water at ambient temperature for at least 24 h to allow complete phase separation.

2.4 Characterization of HNTs

Thermogravimetric analysis (TGA) was carried out using a TG-DTA, DT-40 system (Shimadzu, Japan). The samples (3 mg) were heated from 0 to 800 °C at 10 °C min^{-1} under flowing nitrogen. The elemental composition was analyzed using energy dispersive X-ray fluorescence spectrometry. Measurements were performed on an Oxford ED 2000 X-ray fluorescence spectrometer with a silver cathode and helium was used as the inert gas. The relative contents of elements were evaluated using XpertEase software in General Condition (high voltage, 25 keV). A FEI model TECNAI G^2 transmission electron microscope (200 kV acceleration voltage) was used to study the microstructure of the samples. The samples for analysis were ground in ethanol and agitated in a glass vial to disperse the particles within the solvent. The suspended particles were transferred to and allowed to dry on a copper grid (400 meshes) coated with a strong carbon film.

2.5 Characterization of the membranes

The membrane hydrophilicity was confirmed by measuring the contact angle formed between the membrane surface and the water. The water contact angle (θ) was measured by using a contact angle goniometer (OCA20, Dataphysics Instruments, Germany) at 25 °C and 50% relative humidity. 1 μL of deionized water was dropped on the top surface and the contact angle between the water and the membrane was measured until no further change was observed. To minimize the experimental error, the contact angle was measured at five random locations for each sample and then the average was reported. The microstructure of the membranes was observed by scanning electron microscopy (SEM) using a JEOL Model JSM-6700F (Tokyo, Japan). The samples were frozen in liquid nitrogen and then fractured. The cross section of the membranes was sputtered with gold, which were viewed with the microscope at 10 kV. To analyze the surface morphology and roughness of the membranes, atomic force microscopy (AFM) was employed using the apparatus DI Nanoscope IIIa (Veeco, USA). The samples were glued on a glass substrate. The membrane surfaces were examined in a scan size of 10 μm × 10 μm. A cross flow system (feed stream flowing tangentially to the membrane surface) was used to characterize the performance of the prepared membrane.

 This journal is © The Royal Society of Chemistry 2015

Published on 12 August 2015. Downloaded on 16/01/2016 12:12:48.

Each membrane with an effective area of 22.2 cm^2 was first pre-pressured at 0.2 MPa for 30 min to obtain a stable flux, and then the pure water flux was recorded at 0.1 MPa and a system temperature of 25 ± 2 °C. Then, PEG 20000 (0.5 g L^{-1}) solution was forced to permeate through the membrane at the same pressure. The permeation flux (J) and rejection (R) were calculated using the following equations:

$$J = \frac{V}{A \times \Delta t} \quad (1)$$

$$\%R = \left(1 - \frac{C_p}{C_f}\right) \times 100\% \quad (2)$$

where V is the volume of permeate pure water (L), A is the effective area of the membrane (m^2), Δt is the permeation time (h), C_p is the permeate concentration and C_f is the feed concentration. The concentrations of PEG 20000 were obtained by using a UV spectrophotometer.

The antibacterial activities of the membranes against *E. coli* were tested by using SEM (JSM-6700F) to study the morphology of the cells on the surface of the membranes. A quantity of 100 μL of 10^6 CFU (colony-forming units) per mL of *E. coli* cells suspended in solution was plated on an LB agar growth plate. After 1 h at 37 °C, the square membranes were gently placed on the top of the inoculated agar plates to allow the cells to interact with the materials. Then the plates were incubated at 37 °C for 12 h. The cells on the membranes were fixed with 2.5% glutaraldehyde and 1% OsO_4 (Fluka). The cells were sputter-coated with gold and then imaged under the SEM to study the morphology of the cells on membranes.

Moreover, the bacteriostasis rate is often used in order to quantitatively analyze the antibacterial activity of membranes. *E. coli* was inoculated in 5 ml of LB liquid nutrient medium and shaken for 12 h at 37 °C. The actual number of cells used for a given experiment was determined by the standard serial dilution method. The membrane samples (*ca.* 0.03 g) were cut and sterilized by autoclaving for 20 min, respectively. To test the antibacterial activity, the membrane samples were added into the 5 ml solution inoculated by about 10^6 CFU per ml of *E. coli*, which were incubated at room temperature. After 24 h, the samples were retrieved from the cultures and washed with normal saline. The wash solution was collected and diluted with deionized water till its concentration became 10^{-3} of the original value. The dilution solution (0.2 ml) was spread onto LB culture medium and all the plates were incubated at 37 °C for 24 h. The number of colonies on the plates was determined by the plate count method and the bacteriostasis rate (BR) was defined by the following equation:

$$BR = \left(\frac{n_0 - n_1}{n_0}\right) \times 100\% \quad (3)$$

where n_0 is the number of colonies on the plates treated with control membranes, and n_1 is the number of colonies on the plates treated with hybrid membranes.

Generally, Cu NPs could be easily oxidized by oxygen in air and copper ions could be released from the oxidized NPs. Therefore, in order to study the loss of Cu NPs from the membranes, the stability of Cu NPs in the membranes was also investigated. The membrane sample (1.0 g) was cut into pieces and immersed in 500 mL of deionized water with continuous stirring at room temperature. Three hours later, the water sample was collected and additional 500 mL of deionized water was added, and the steps were repeated. The concentrations of copper ions were analyzed with an ICP AES machine (ICP, Iris Advantage 1000).

3. Results and discussion

3.1 Characterization of HNTs

In order to obtain the grafted amount of P4VP, the TGA curves of HNTs (a), HNTs modified by CPS (b), and P4VP grafted HNTs at different reaction times, namely 3, 6, 9, and 12 h (c–f), are shown in Fig. 2. As can be seen from Fig. 2a, one major mass loss was observed in the temperature range of 0–150 °C, corresponding to the loss of adsorbed water (surface and interlayer).[24] Another mass loss in the range 450–550 °C was assigned to the dehydroxylation of structural AlOH groups of HNTs.[24,25] For HNTs modified by CPS (Fig. 2b), there was a new weight loss between 300 and 450 °C as compared with raw HNTs, which was due to the decomposition of the grafted CPS. For P4VP grafted HNTs at different times, 3, 6, 9, and 12 h (c–f), the new weight loss between 300 and 375 °C corresponded to the decomposition of the grafted P4VP. The grafted amount of P4VP could be obtained according to the following equation:

$$\text{Grafted amount} = \frac{\Delta w}{1 - \Delta w} \quad (4)$$

Herein, Δw is the weight loss. Therefore, the grafted amounts of P4VP at different times, 3, 6, 9, and 12 h, were 0.12, 0.16, 0.26 and 0.32 g of P4VP per g of HNTs, respectively.

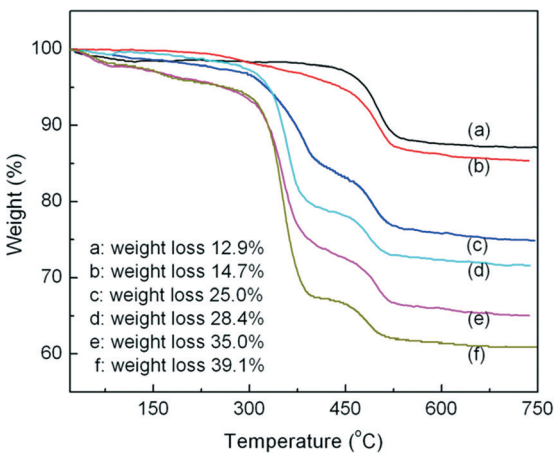

Fig. 2 TGA curves of HNTs (a), HNTs modified by CPS (b), and P4VP grafted HNTs at different reaction times, namely 3, 6, 9, and 12 h (c–f).

Published on 12 August 2015. Downloaded on 16/01/2016 12:12:48.

Table 1 Surface elemental composition of Cu NPs@HNTs *via* X-ray fluorescence spectrometry

	Element concentration (wt%)					
	Al	Si	S	K	Fe	Cu
Cu NPs@HNTs	11.00	13.79	0.618	0.152	0.497	6.513

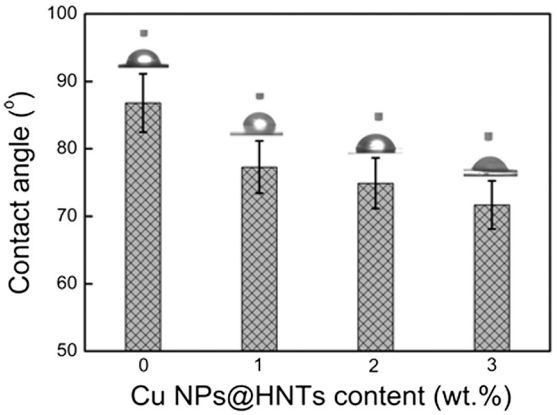

Fig. 3 Water contact angles of PES membranes containing various Cu NPs@HNT contents.

The microstructures of HNTs and Cu NPs@HNTs were observed by TEM and the results are shown in Fig. 1b and c. As can be seen from Fig. 1b, HNTs, a type of natural nanotube, have a cylindrical shape and contain a transparent central area that runs longitudinally along the cylinder, indicating that the nanotubular particles are hollow and open-ended, with a length of 0.5–2 μm and an inner diameter of 20–30 nm. The shell thickness is 15–20 nm.[26,27] The large and smooth unhindered pores can provide a sufficient water channel, which could remarkably improve the water flux of the membranes if the HNTs could be dispersed uniformly in the membrane matrix. Fig. 1c clearly shows that Cu NPs appear uniformly distributed across the surface of HNTs and the average diameter is about 10 nm, indicating that Cu NPs have been successfully loaded onto the HNT surface. Table 1 gives the surface element composition of Cu NPs@HNTs. Three typical elements including Si, Al, and Cu were observed and attributed to HNTs and Cu NPs. The composition of Cu is 6.513 wt%.

3.2 Characterization of the membranes

The water contact angle measurement is used to characterize the hydrophilic properties of the membrane surface and the results are shown in Fig. 3. The contact angle of the membranes decreased gradually with the increase of Cu NPs@HNT content and decreased to as low as 71.7° with 3.0 wt% Cu NPs@HNTs. It was well established that a lower contact angle corresponded to a better hydrophilicity, thus notably indicating that the hybrid membranes presented an enhanced hydrophilicity with an increase in Cu NPs@HNT amount. The explanation is as follows: during the formation of hybrid membranes, most of the hydrophilic Cu NPs@HNTs tend to migrate toward the top layer of the membrane so as to decrease the interface energy. Therefore, the hydrophilic Cu NPs@HNTs originated from the membrane surface were easily wetted and adsorbed by water, giving rise to a lower water contact angle. Some related research

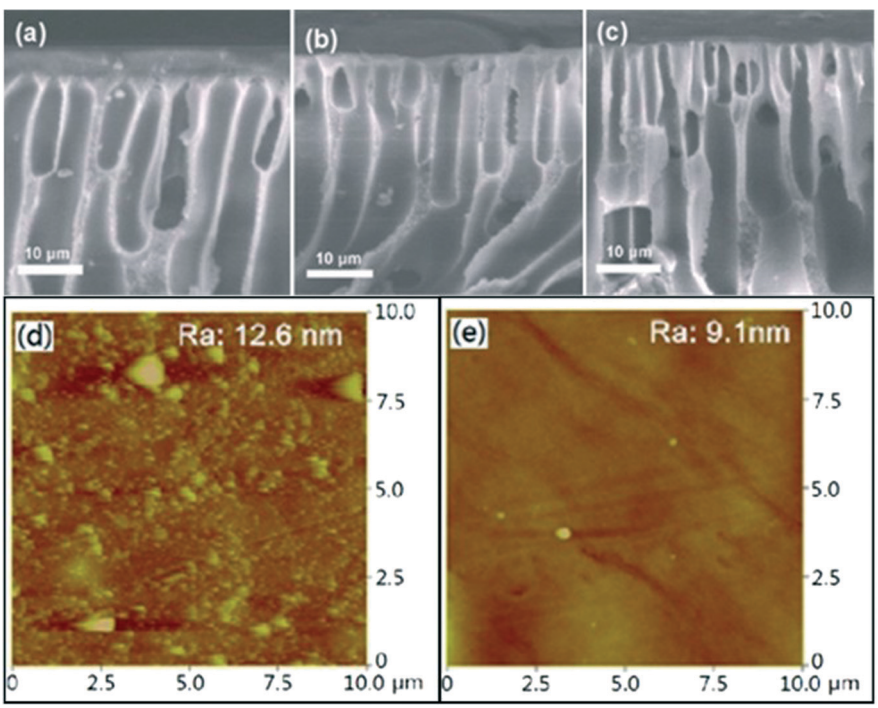

Fig. 4 SEM images of the cross-section morphology of membranes: (a) pure PES membrane, (b) 1.0 wt% Cu NPs@HNTs/PES membrane, and (c) 3.0 wt% Cu NPs@HNTs/PES membrane. AFM surface images of the membranes: (d) pure PES membrane and (e) 3.0 wt% Cu NPs@HNTs/PES membrane.

 This journal is © The Royal Society of Chemistry 2015

Published on 12 August 2015. Downloaded on 16/01/2016 12:12:48.

studies reported similar phenomena for the additive of graphene oxide (GO) and carbon nanotubes (CNTs).[28,29]

Fig. 4a–c show the SEM images of the pure PES membrane and the hybrid membranes with Cu NPs@HNT contents of 1.0 wt% and 3.0 wt%, respectively. All the membranes had a similar asymmetric structure, which was the typical structure of ultrafiltration membranes, with a top dense layer, a porous sublayer, and fully developed macropores at the bottom.[30] These findings indicated that the addition of Cu NPs@HNTs could not affect the microstructures of the membranes. However, compared with the pure PES membrane, the thickness of the top dense layer decreased with the increase in Cu NPs@HNT content, which could be explained by the fact that the addition of hydrophilic Cu NPs@HNTs increased the thermodynamic instability of the casting solution and accelerated the phase separation. Fig. 4d and e display the three-dimensional AFM images of the membrane surfaces. It can be seen that the surface of the hybrid membrane (containing 3 wt% Cu NPs@HNTs) was smoother than the control PES membrane. Furthermore, the mean roughness (R_a) of the membranes decreased from 12.6 nm for the pure membrane to 9.1 nm for the hybrid membrane. The membrane with lower roughness and surface energy has stronger antifouling ability. Therefore, it is important to fabricate a membrane with low surface energy and roughness to improve the antifouling ability and performance of the membrane.

The effect of Cu NPs@HNT content on the pure water flux and the rejection of PEG 20000 are shown in Fig. 5. The pure water flux reached a maximum as high as 212 L m^{-2} h^{-1} when the Cu NPs@HNT content was 2.0 wt%. When the Cu NPs@HNT content increased up to 3.0 wt%, the flux was still higher than that of the pure PES membrane. The improved flux is mainly because of the increase in the hydrophilicity (see Fig. 3) and the thinner layer surface (see Fig. 4a–c). However, the water flux of the membrane containing 3.0 wt% Cu NPs@HNTs decreased, although the hydrophilicity also improved. The results could be explained by the fact that when the Cu NPs@HNT content was 3.0 wt%, the phase separation was accelerated, and the top layer became denser, resulting in a decrease in flux. There were no apparent differences between the rejections for all the membranes; the rejections were kept above 80%.

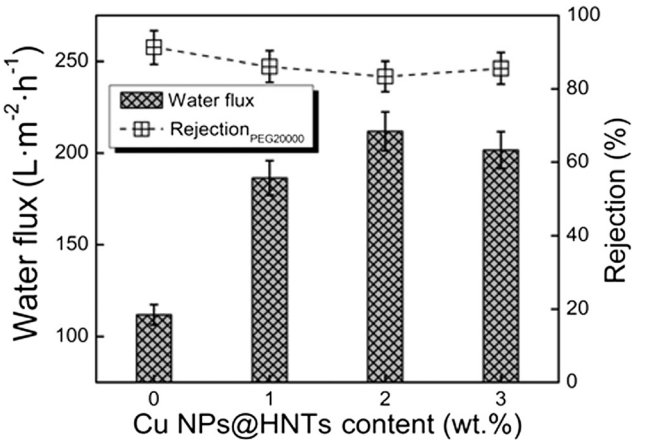

Fig. 5 Separation performance of PES membranes containing various Cu NPs@HNT contents.

The antibacterial activity of the membranes against *E. coli* was tested by using SEM to study the morphology of the cells on the surface of the membranes, and the results are shown in Fig. 6a and b. Fig. 6a reveals that the surface morphology of the *E. coli* cells on the pure PES membrane was intact, peritrichous and rod-shaped, indicating that the PES membrane had no antibacterial activity. In contrast, the morphology of a large fraction of *E. coli* cells on the hybrid membrane was obviously damaged in Fig. 6b. The bacteriostasis rate was used to quantitatively analyze the antibacterial activity of the test membranes by the viable cell counting technique. As shown in Fig. 6c and d, the number of colonies on the plates

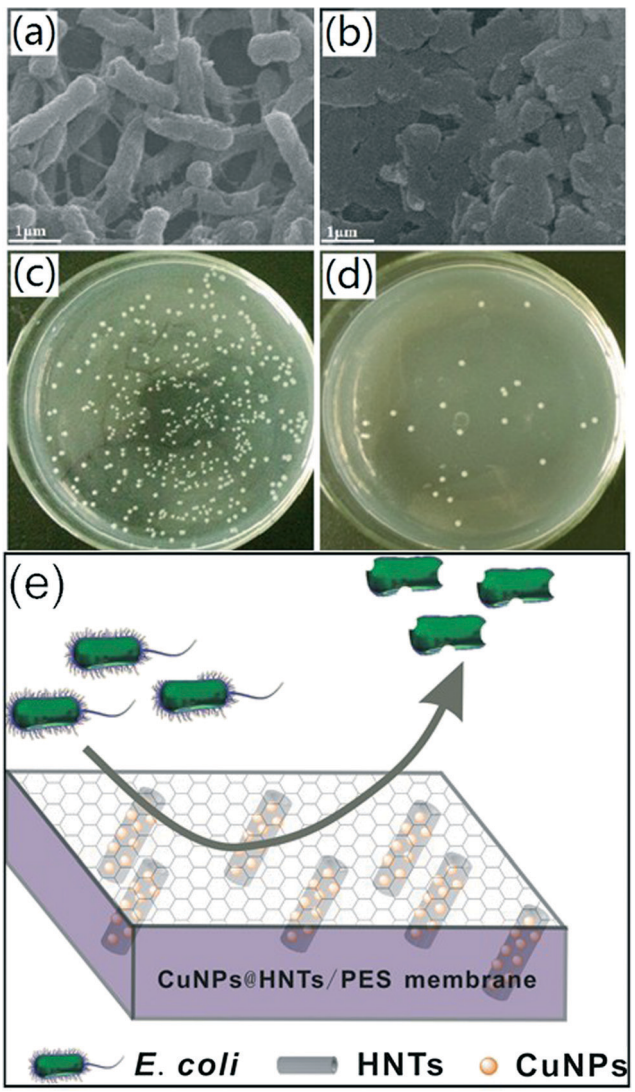

Fig. 6 SEM images of *E. coli* attached to membranes: (a) PES membrane and (b) 3.0 wt% Cu NPs@HNTs/PES membrane (12 h incubation at 37 °C); measurement of antibacterial activity of membranes by the bacteriostasis rate: (c) PES membrane and (d) 3.0 wt% Cu NPs@HNTs/PES membrane; (e) schematic illustration of the antibacterial mechanism of Cu NPs@HNTs/PES hybrid membranes.

Published on 12 August 2015. Downloaded on 16/01/2016 12:12:48.

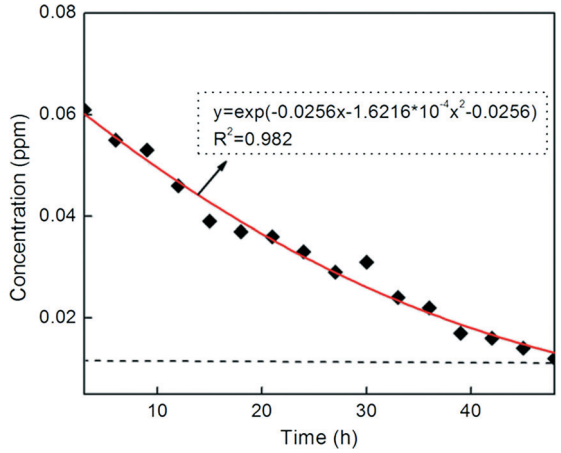

Fig. 7 Leaching test results for the PES membrane containing 3.0 wt% Cu NPs@HNTs (copper concentration in the leaching solution *versus* leaching time).

treated with Cu NPs@HNTs/PES hybrid membranes decreased significantly with a high bacteriostasis rate against *E. coli* of 94.5%. The higher bacteriostasis rate demonstrates better antibacterial ability and the above results suggest that the Cu NPs@HNTs/PES membrane has a preferable antibacterial ability which is reasonably attributed to the introduction of Cu NPs@HNT nanomaterials.

Copper nanoparticles could attach to the bacterial cell membrane, causing structural changes or functional damage and inhibiting its growth, leading to cell death.[13] Another more important mechanism of action has been proposed wherein the dissipation of cell membrane potential due to the formation of cell filaments and reactive oxygen species (ROS) can damage the bacterial cell membrane and bacterial DNA, which can cause protein oxidation and result in bacterial cell death.[31] A schematic illustration of the antibacterial mechanism of the hybrid membranes is shown in Fig. 6e.

The results from the leaching tests for Cu NPs in the membranes are presented in Fig. 7. It is observed that the immobilized Cu NPs on the membranes were leached out and the concentration in the leaching solution decreased with time; after that the leaching of Cu NPs was no longer detected. The immobilized Cu NPs on the membranes could reach a stable value within a shorter time. Besides, the maximum value for the concentration in the leaching solution was only 0.06 ppm. The results indicate that the leaching of Cu NPs could not result in secondary pollution, leading to potential applications in water purification or separation of protein and peptide.

4. Conclusions

The antibacterial behavior of halloysite nanotubes decorated with copper nanoparticles in a novel mixed matrix membrane for water purification has been investigated. Compared with virgin membranes, the membranes functionalized by halloysite nanotubes decorated with copper nanoparticles showed excellent water flux and antibacterial activity. More importantly, the copper nanoparticles in the membrane matrix are more stable and could not cause secondary pollution. Therefore, the above membranes have a wide range of potential applications in the treatment of direct or indirect potable water.

Acknowledgements

This work was financially sponsored by the National Natural Science Foundation of China (no. 21106137 and 21376225). We sincerely acknowledge the financial assistance of the visiting research program in the University of New South Wales by the China Scholarship Council (no. 201208410135).

References

1 K. Boussu, C. Vandecasteele and B. Vander, Study of the characteristics and the performance of self-made nanoporous polyethersulfone membranes, *Polymer*, 2006, **47**, 3464–3476.
2 A. Razmjou, J. Mansouri and V. Chen, The effects of mechanical and chemical modification of TiO_2 nanoparticles on the surface chemistry, structure and fouling performance of PES ultrafiltration membranes, *J. Membr. Sci.*, 2011, **378**, 73–84.
3 C. Hessel, V. Pattani, M. Rasch, M. Panthani, B. Koo, J. Tunnell and B. Korgel, Copper Selenide Nanocrystals for Photothermal Therapy, *Nano Lett.*, 2011, **11**, 2560–2566.
4 J. J. Qin, M. H. Oo and Y. Li, Development of high flux polyethersulfone hollow fiber ultrafiltration membranes from a low critical solution temperature dope *via* hypochlorite treatment, *J. Membr. Sci.*, 2005, **247**, 137–142.
5 P. Gunawan, C. Guan, X. Song, Q. Zhang, S. S. Leong, C. Tang, Y. Chen, M. B. Chan-Park, M. W. Chang, K. Wang and R. Xu, Hollow Fiber Membrane Decorated with Ag/MWNTs: Toward Effective Water Disinfection and Biofouling Control, *ACS Nano*, 2011, **5**, 10033–10040.
6 J. Li, Z. Xu, H. Yang, L. Yu and M. Liu, Effect of TiO_2 nanoparticles on the surface morphology and performance of microporous PES membrane, *Appl. Surf. Sci.*, 2009, **255**, 4725–4732.
7 M. Luo, J. Zhao, W. Tang and C. Pu, Hydrophilic modification of poly (ether sulfone) ultrafiltration membrane surface by self-assembly of TiO_2 nanoparticles, *Appl. Surf. Sci.*, 2005, **249**, 76–84.
8 J. Shen, H. Ruan, L. Wu and C. Gao, Preparation and characterization of PES-SiO_2 organic–inorganic composite ultrafiltration membrane for raw water pretreatment, *Chem. Eng. J.*, 2011, **168**, 1272–1278.
9 V. Vatanpour, S. Madaeni, L. Rajabi, S. Zinadini and A. Derakhshan, Boehmite nanoparticles as a new nanofiller for preparation of antifouling mixed matrix membranes, *J. Membr. Sci.*, 2012, **401–402**, 132–143.
10 J. Zhang, Y. Zhang, Y. Chen, S. Yi, B. Zhang, H. Zhang and J. Liu, Preparation and characterization of PES/HNTs hybrid ultrafiltration membranes, *Adv. Sci. Lett.*, 2012, **11**, 57–62.
11 E. Celik, H. Park, H. Choi and H. Choi, Carbon nanotube blended polyethersulfone membranes for fouling control in water treatment, *Water Res.*, 2011, **45**, 274–282.

 This journal is © The Royal Society of Chemistry 2015

Published on 12 August 2015. Downloaded on 16/01/2016 12:12:48.

12 L. Esteban-Tejeda, F. Malpartida, A. Esteban-Cubillo, C. Pecharroman and J. Moya, Antibacterial and antifungal activity of a soda-lime glass containing copper nanoparticles, *Nanotechnology*, 2009, **20**, 505701.
13 X. Ding, H. Wang, W. Chen, J. Liu and Y. Zhang, Preparation and antibacterial activity of copper nanoparticles/halloysite nanotubes nanocomposites *via* reverse atom transfer radical polymerization, *RSC Adv.*, 2014, **4**, 41993–41996.
14 Y. Zhang, Y. Chen, H. Zhang, B. Zhang and J. Liu, Potent antibacterial activity of a novel silver nanoparticle-halloysite nanotubes nanocomposite powder, *J. Inorg. Biochem.*, 2013, **118**, 59–64.
15 L. Yu, Y. Zhang, B. Zhang and J. Liu, Enhanced antibacterial activity of silver nanoparticles/halloysite nanotubes/graphene nanocomposites with sandwich-like structure, *Sci. Rep.*, 2014, **4**, 4551.
16 J. Drelich, B. Li, P. Bowen, J. Y. Hwang, O. Mills and D. Hoffman, Vermiculite decorated with copper nanoparticles: Novel antibacterial hybrid material, *Appl. Surf. Sci.*, 2011, **257**, 9435–9443.
17 Y. Lvov, D. Shchukin, H. Möhwald and R. Price, Halloysite clay nanotubes for controlled release of protective agents, *ACS Nano*, 2008, **2**, 814–820.
18 Y. Lvov and E. Abdullayev, Green and functional polymer-clay nanotube composites with sustained release of chemical agents, *Prog. Polym. Sci.*, 2013, **38**, 1690–1719.
19 C. Liu, L. Yu, Y. Zhang, B. Zhang, J. Liu and H. Zhang, Preparation of poly(sodium acrylate-acrylamide) superabsorbent nanocomposites incorporating graphene oxide and halloysite nanotubes, *RSC Adv.*, 2013, **3**, 13756–13763.
20 J. Qiu, Y. Zhang, Y. Zhang, H. Zhang and J. Liu, Synthesis and antibacterial activity of copper-immobilized membrane comprising grafted poly (4-vinylpyridine) chains, *J. Colloid Interface Sci.*, 2011, **354**, 152–159.
21 C. Wan, M. Li, X. Bai and Y. Zhang, Synthesis and characterization of photoluminescent Eu (III) coordination halloysite nanotube-based nanohybrids, *J. Phys. Chem. C*, 2009, **113**, 16238–16246.
22 J. Jiang, Y. Zhang, D. Cao and P. Jiang, Controlled immobilization of methyltrioxorhenium (VII) based on SI-ATRP of 4-vinyl pyridine from halloysite nanotubes for epoxidation of soybean oil, *Chem. Eng. J.*, 2013, **215–216**, 222–226.
23 Y. Chen, Q. Deng, J. Xiao, H. Nie, L. Wu, W. Zhou and B. Huang, Controlled grafting from poly(vinylidene fluoride) microfiltration membranes *via* reverse atom transfer radical polymerization and antifouling properties, *Polymer*, 2007, **48**, 7604–7613.
24 J. Zhang, Y. Zhang, Y. Chen, L. Du, B. Zhang, H. Zhang, J. Liu and K. Wang, Preparation and characterization of novel polyethersulfone hybrid ultrafiltration membranes bending with modified halloysite nanotubes loaded with silver nanoparticles, *Ind. Eng. Chem. Res.*, 2012, **51**, 3081–3090.
25 Y. Chen, Y. Zhang, J. Liu, H. Zhang and K. Wang, Preparation and antibacterial property of polyethersulfone ultrafiltration hybrid membrane containing halloysite nanotubes loaded with copper ions, *Chem. Eng. J.*, 2012, **210**, 298–308.
26 H. Yu, Y. Zhang, X. Sun, J. Liu and H. Zhang, Improving the antifouling property of polyethersulfone ultrafiltration membrane by incorporation of dextran grafted halloysite nanotubes, *Chem. Eng. J.*, 2014, **237**, 322–328.
27 Y. Chen, Y. Zhang, H. Zhang, J. Liu and C. Song, Biofouling control of halloysite nanotubes-decorated polyethersulfone ultrafiltration membrane modified with chitosan-silver nanoparticles, *Chem. Eng. J.*, 2013, **228**, 12–20.
28 V. Vatanpour, S. S. Madaeni, R. Moradian, S. Zinadini and B. Astinchap, Fabrication and characterization of novel antifouling nanofiltration membrane prepared from oxidized multiwalled carbon nanotube/polyethersulfone nanocomposite, *J. Membr. Sci.*, 2011, **375**, 284–294.
29 V. Vatanpour, S. S. Madaeni, R. Moradian, S. Zinadini and B. Astinchap, Preparation of a novel antifouling mixed matrix PES membrane by embedding graphene oxide nanoplates, *J. Membr. Sci.*, 2014, **453**, 292–301.
30 M. Sun, Y. Su, C. Mu and Z. Jiang, Improved Antifouling Property of PES Ultrafiltration Membranes Using Additive of Silica-PVP Nanocomposite, *Ind. Eng. Chem. Res.*, 2010, **49**, 790–796.
31 A. K. Chatterjee, R. Chakraborty and T. Basu, Mechanism of antibacterial activity of copper nanoparticles, *Nanotechnology*, 2014, **25**, 135101.